Pareto-based design optimization of chemical tank farm using a trade-off between domino effects related and land resource utilization efficiency

Men, Jinkun; Chen, Guohua; Reniers, Genserik

DOI
10.1016/j.ress.2024.110203

Publication date
2024

Document Version
Final published version

Published in
Reliability Engineering and System Safety

Citation (APA)
Men, J., Chen, G., & Reniers, G. (2024). Pareto-based design optimization of chemical tank farm using a trade-off between domino effects related and land resource utilization efficiency. *Reliability Engineering and System Safety*, *249*, Article 110203. https://doi.org/10.1016/j.ress.2024.110203

Reliability Engineering and System Safety 249 (2024) 110203

Contents lists available at ScienceDirect

Reliability Engineering and System Safety

journal homepage: www.elsevier.com/locate/ress

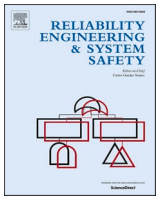

Pareto-based design optimization of chemical tank farm using a trade-off between domino effects related and land resource utilization efficiency

Jinkun Men [a,b,c], Guohua Chen [a,b,*], Genserik Reniers [c,d,e]

[a] Institute of Safety Science & Engineering, South China University of Technology, Guangzhou 510640, China
[b] Guangdong Provincial Science and Technology Collaborative Innovation Center for Work Safety, Guangzhou 510640, China
[c] CEDON, KU Leuven, Campus Brussels, Brussels 1000, Belgium
[d] Faculty of Technology, Policy and Management, Safety and Security Science Group (S3G), TU Delft, 2628 BX, Delft, the Netherlands
[e] Faculty of Applied Economics, Antwerp Research Group on Safety and Security (ARGoSS), University Antwerp, Antwerp 2000, Belgium

ARTICLE INFO

Keywords:
Chemical tank farm design
Inherent safety design
Safety and economy
Pareto-based optimization
Parametric risk analysis

ABSTRACT

Industrial production intensification greatly enhances resource utilization efficiency and production efficiency within the modern petrochemical industry (MPI). However, densely located hazardous installations pose significant threats to workers, society and environment. Under this impetus, an advanced pareto-based optimization methodology is proposed for chemical tank farm (CTF) design. The objectives of domino risk minimization and land resource utilization efficiency maximization can be achieved through optimizing the locations and dimensions of storage tanks. A simplified quantitative domino risk assessment procedure is developed within a grid-based Cartesian coordinate system, which links the design parameters and risk values. A bi-objective optimization model is developed for problem formulation and a well-designed simulated annealing-based multi-objective particle swarm optimization is proposed for model solving. A CTF with six floating roof diesel tanks is adopted for case study. The simulated annealing-based jumping mechanism can effectively avoid the local optimum, which makes the algorithm easier to obtain the trade-off with great convergence and diversity. The proposed methodology can provide safer and more cost-effective design solutions. Results indicate that the design parameters can significantly affect the regional domino risk distribution. The conflicting nature between safety and economy is discussed. This work is of great significance for the safety and reliability of MPI.

1. Introduction

The petrochemical industry holds a significant position in the global economy, which is one of the indispensable parts of modern society [1]. In line with the trend of industrial production intensification, a large number of chemical industrial parks (CIPs) have been established in China in recent years [2]. To enhance resource utilization efficiency, production efficiency and other benefits of scale, CIPs exist to concentrate different chemical-related activities [3,4]. However, due to the flammable, explosive, and toxic characteristics of hazardous chemicals, densely located hazardous installations also cause a series of safety and security issues [5-9].

On April 17, 2013, an ammonium nitrate explosion occurred at the West Fertilizer Company in Texas, resulting in 15 deaths [10]. On March 21, 2019, a major explosion occurred at a chemical plant in Xiangshui, Jiangsu, resulting in 78 deaths and direct economic losses amounting to 1.986 billion RMB [11]. On August 4, 2020, two major explosions occurred at the port of Beirut, Lebanon, resulting in at least 220 deaths and economic losses of approximately 15 billion dollars [12]. Since the petrochemical industry involves manifold high-risk chemical processes, safety is one of the key pillars of sustainable development [13-15].

As reported by numerous studies [3,16,17], catastrophic chemical accidents occur frequently around the world, which have imposed tremendous challenges on society, environment, and economy. More alarmingly, once fires or explosions occur, subsequent accidents (so called domino events) may be easily triggered due to the congestion of hazardous installations [18,19]. Over the past few decades, continuous efforts have been made in the research on domino accidents prevention & mitigation [4]. An external domino accident prevention framework (denoted as *Hazwim*) was proposed by Reniers et al. [20], which integrates *HAZOP, What-If Analysis* and *Risk Matrix* into an effective standardized risk analysis framework. Jia et al. [21] developed a

* Corresponding author at: South China University of Technology, No.381, Wushan Rd., Tianhe District, Guangzhou 510640, China.
E-mail address: mmghchen@scut.edu.cn (G. Chen).

https://doi.org/10.1016/j.ress.2024.110203
Received 1 December 2023; Received in revised form 7 April 2024; Accepted 13 May 2024
Available online 14 May 2024

Table 1
Overview of representative studies for accident prevention & mitigation.

Ref.	Methodology	Stages	Main work
[24]	Risk Matrix	Design	A risk-based methodology was proposed to guide the application of fireproofing.
[25]	Deep Learning	Production and Operation	A fuzzy deep neural network was proposed for early warning of industrial accidents.
[26]	Cost Benefit Analysis	Production and Operation	Focusing on potential environmental and eco-terroristic attacks in chemical facilities, an economic model was proposed to allocate preventive security measures.
[27]	Dynamic Graph	Production and Operation	A dynamic graph approach was developed to integrate safety and security resources for reducing the risk of man-made domino effects.
[28]	Multi-objective Optimization	Emergency Response	A multi-objective emergency facilities location methodology was proposed for domino accidents in CIP.
[29]	Multi-objective optimization	Design	A multi-objective optimization method was proposed for industrial park layout design.
[30]	Inherent Safety Design	Design	Inherent safety design tools were developed based on the quantitative risk assessment (QRA) as a benchmark.
[31]	Petri-net	Emergency Response	A Petri-net based cooperation modeling approach was proposed for emergency response time analysis.
[32]	Cost-effectiveness Optimization	Production and Operation	A cost-effectiveness safety investment optimization approach was proposed for domino effect risk reduction.
[33]	Petri-net	Emergency Response	A Petri-net approach was proposed to optimize firefighting force allocation, which can prevent the escalation of fire included domino accidents.
[34]	Multi-objective Optimization	Emergency Response	A goal programming-based multi-objective optimization approach was proposed to identify the optimal firefighting strategies in domino accidents.
[35]	Cost-effectiveness Optimization	Production and Operation	A cost-effectiveness optimization approach was proposed to support the decision-making on safety barrier establishments and improvements.
[15]	Path Optimization	Emergency Response	A risk-based evacuation planning method was proposed for domino accidents in CIPs.
[36]	Path Optimization	Emergency Response	An evacuation path planning method was proposed for multi-hazard accidents in CIPs.

five-level domino accident prevention framework, of which a systematic macro-integration is provided to efficiently utilize multiple safety measures. Zeng et al. [22] developed a systematic safety barrier management framework to cope with domino effects, of which the prevention and mitigation strategies using safety barriers are explored in the form of a bow-tie diagram. Following the idea of chain-cutting disaster mitigation, Yang et al. [23] proposed a full-life cycle domino accidents mitigation system, which mainly consists of five stages: site selection and layout, design, production and operation, emergency response, and post-disaster recovery.

In addition to the systematic frameworks mentioned above, a wide variety of specific methodologies have also been developed to cope with chemical accidents, see Table 1. As shown, most of accident prevention & mitigation strategies were proposed for the stages of Production and Operation and Emergency Response. From the perspective of process risk management, accident prevention & mitigation strategies can be divided into three categories: inherent safety design, domino effects avoidance, and add-on safety & procedural safety [30,37]. The evolution of domino accidents exhibits an increasing trend [19,38]. According to the chain-cutting disaster mitigation theory [23], the most effective accident prevention & mitigation should involve stopping accidents from occurring or escalating at an early stage or before they occur. Therefore, strategies for the site selection and design stages are particularly important. Inherent safety design (ISD) can be regarded as one of the most effective accident prevention & mitigation strategies, which seeks to eliminate or at least reduce the hazard involved in the chemical process at its source [13,30,39].

Parameterized ISD methods are often limited by deviations in inherent safety indicators and the inability to quantify potential accident scenarios and consequences. To recognize the logical relationship between design parameters and potential accident scenarios, Zhu et al. [30] incorporated the quantitative risk assessment (QRA) into the inherent safety design. At present, QRA has been wildly regarded as the benchmark to develop safety decision making methods [15,40,41]. As one of the core tasks in process safety, risk analysis plays a crucial role in preventing and migrating fatalities, asset and reputation loss caused by accidents [42,43]. Since the publication of the *Guidelines for Chemical Process Quantitative Risk Analysis* [44], the QRA framework has garnered significant attention. The first systematic QRA procedure for domino accidents was proposed by Cozzani et al. [45], of which risk is quantified by the product of accident probability and accident consequences. However, it is still challenging to establish a parameterized optimization function through the existing QRA procedure, which hinders optimization algorithms from exploring a wide range of the feasible solution domain.

Moreover, practical safety decision making faces complexity due to multi-dimensional dependence and conflicting factors [40]. Decision making in safety and economy is confronted with different conflicting objectives, which can be referred to a multi-objective problem (MOP) [28,46,47]. As mentioned by Khan et al., [40], there are only a few studies that consider the conflicting nature between different objectives. Even as safety-critical systems, the fundamental purpose of high-risk industrial activities remains to generate significant profits. Thus, a safety-critical system should be designed by presenting an optimal decision in terms of efficiency, economics, and safety among various alternatives [48,49].

Under this impetus, this work developed a Pareto-based optimization methodology for a parameterized chemical tank farm design problem. The contributions and novelties of this work are mainly reflected in four aspects.

(1) An advanced pareto-based chemical tank farm design methodology is proposed for domino risk minimization and land resource utilization efficiency maximization. A parameterized ISD tool is available to achieve a trade-off between safety and economy, thereby enhancing the safety and reliability of the system in a more sustainable and realistic manner.
(2) On the basis of the QRA framework, a simplified quantitative domino risk assessment procedure (S-QRA) is developed within a grid-based Cartesian coordinate system, which links the design parameters and risk values. Compared with traditional inherent safety indicators, S-QRA provides a more comprehensive safety decision optimization preference benchmark, as it can systematically quantify multiple uncertainties caused by probabilities and consequences of potential industrial accidents and corresponding domino effects.
(3) A well-designed simulated annealing-based multi-objective particle swarm optimization is proposed for model solving. To cope with the fragmentation of feasible solution space caused by complex model constraints, the simulated annealing process

Algorithm 1
Simplified quantitative domino risk assessment procedure.

Input: Basic Information Set Φ_{set}; Scale Factor Δ; Risk Threshold μ; Basic Failure Frequency P_{bf}; Tank Set $\mathscr{T}$
Output: Risk Distribution Matrix $\mathscr{R}_{N\times M}$; High-risk Area $\mathscr{A}$
Initialization Module:
Cartesian Coordinate System Construction: $\Theta(x,y)\leftarrow Meshing(\Phi_{\text{set}},\Delta), x\in[0,M], y\in[0,N]$
Distance Matrix Calculation: $\mathscr{D}^1_{|\mathscr{T}|\times|\mathscr{T}|}\leftarrow pdist(\{(x_t,y_t)|t\in\mathscr{T}\})$; $\mathscr{D}^2_{N\times M\times|\mathscr{T}|}\leftarrow pdist(\Theta(x,y)), x,y\in Z^+$
Accident Consequence Modeling: $\mathscr{I}^1=(I_{ij})_{|\mathscr{T}|\times|\mathscr{T}|}\leftarrow FER(\mathscr{D}^1,\Phi_{\text{set}})$; $\mathscr{I}^2=(I_{t,(x,y)})_{N\times M\times|\mathscr{T}|}\leftarrow FER(\mathscr{D}^2,\Phi_{\text{set}}), x,y\in Z^+$
Domino Probability Calculation: $\mathscr{P}^{do}=\left(P^{do}_{i,j}\right)_{|\mathscr{T}|\times|\mathscr{T}|}\leftarrow ProbitDo(\mathscr{I}^1,\Phi_{\text{set}})$
Death Probability Calculation: $\mathscr{P}^{de}=\left(P^{de}_{t,(x,y)}\right)_{N\times M\times|\mathscr{T}|}\leftarrow ProbitDe(\mathscr{I}^2,\Phi_{\text{set}}), x,y\in Z^+$
Risk Superposition Module:
For *all integer coordinate points* $(x,y)\in\Theta, x,y\in Z^+$ ***Do***
$Risk(x,y)=0$
For *all tank* $t\in\mathscr{T}$ ***Do***

$$Risk(x,y)=Risk(x,y)+P_{bf}\times\left[P^{de}_{t,(x,y)}+\sum_{j\in\mathscr{T},j\neq t}\left(P^{do}_{t,j}\times P^{de}_{j,(x,y)}\right)\right]$$

End For
End For
High-risk Area Identification Module:
Risk Distribution Matrix Construction: $\mathscr{R}=(Risk(x,y))_{N\times M}, x\in Z^+(0,M], y\in Z^+(0,N]$
Risk Contour Calculation: $\ell,\mathscr{A}\leftarrow contour(\mathscr{R},\Theta,\mu)$

gives the algorithm controllable probabilities of accepting inferior solutions, which can effectively avoid falling into the local optimum. Analysis results indicate that the proposed algorithm is competitive in terms of diversity and convergence.

(4) The conflicting nature between domino risk and land resource utilization efficiency is discussed. Even though chemical tank farm design is the main motivation of this work, the proposed methodology is not limited to this, as many safety-critical system design problems face similar challenges.

The rest of this work is stated as follows. In Section 2, preliminaries are stated to clarify S-QRA. Model formulation and solving strategy are stated in Section 3. Section 4 gives a case study to demonstrate the proposed pareto-based optimization methodology. The conflicting nature of safety and economy is discussed in Section 5. At last, the work is concluded in Section 6. Other basic information is stated in the Appendix.

2. Preliminaries

2.1. General procedure

A simplified quantitative domino risk assessment procedure is developed in this section. The general procedure of S-QRA is shown in the pseudocode Algorithm 1, which consists of three modules, i.e., *initialization module, risk superposition module*, and the *high-risk area identification module*. The inputs of S-QRA procedure mainly include the basic information set Φ_{set} (geographical and meteorological information, material characteristics, tank characteristics, etc.), scale factor Δ, risk threshold μ, basic failure frequency of chemical tank P_{bf}. The risk threshold μ and the basic failure frequency of the chemical tank "P_{bf}" can be extracted from the Appendix, Tables A.1 and B.1.

The **initialization module** primarily focuses on the processing of basic information set Φ_{set}, including (1) cartesian coordinate system construction, (2) distance matrix calculation, (3) accident consequence modeling, (4) death probability calculation. Following the Chinese Standard GB 36,894–2018 [50] and QRA framework [45], the **risk superposition module** superimposes the individual risk caused by all tank units in the chemical tank farm, and can obtain the risk value of any geographical location in the area. Individual risk is defined as [45,50]: the frequency of death due to hazardous chemical accidents assuming that a person is in a certain place for a long time without any protective measures. On the basis of the cartesian coordinate system, risk values of all integer coordinate points are regarded as the corresponding elements of the risk distribution matrix. As a result, the **high-risk area identification module** can identify the high-risk regions where the

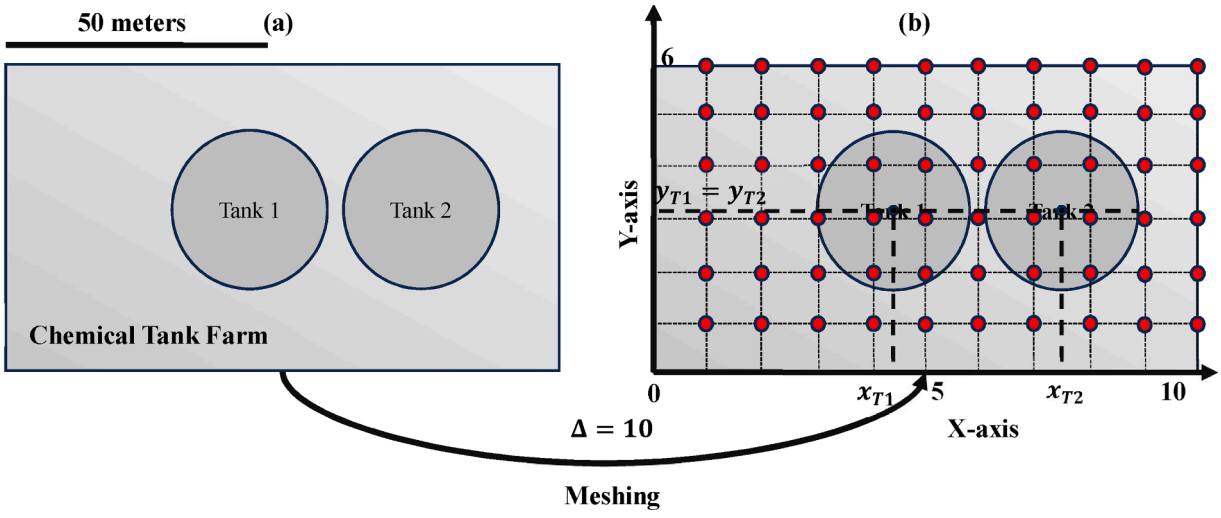

Fig. 1. Illustration of the constructed cartesian coordinate system.

corresponding risk value is greater than the risk threshold. The total area of high-risk regions is adopted as the safety decision optimization preference benchmark.

In this work, various risk-related information is integrated into the cartesian coordinate system, such as tank farm layout, accident consequences, personnel death probability, domino escalation probability, etc. The core of the S-QRA procedure is to convert the regional risk distribution to a matrix through discrete coordinate points, which provides great convenience for optimization calculations. Through the S-QRA procedure, the risk distribution matrix $\mathscr{R}_{\boldsymbol{N}\times\boldsymbol{M}}$ and high-risk area $\mathscr{A}$ can be obtained. Compared with the traditional QRA framework, the S-QRA procedure can provide a mapping relationship between decision variables and optimization objective function by linking design parameters and domino risk values.

2.2. Initialization module

2.2.1. Cartesian coordinate system

To integrate various risk-related information, a cartesian coordinate system is constructed to model the chemical tank farm.

A chemical tank farm measuring 100 m in length and 60 m in width is shown in Fig. 1(a). Suppose that the scale factor Δ is 10 m, the cartesian coordinate system $\Theta(x,y), x\in[0,10], y\in[0,6]$ is shown in Fig. 1 (b). The x-axis and y-axis constitute the Cartesian coordinate system. The locations of Tank 1 and Tank 2 are represented by the coordinates of their center points (x_{T1},y_{T1}) and (x_{T2},y_{T2}). The distance between any two points in the cartesian coordinate system can be calculated by their coordinates.

$$d_{ij}=\Delta\sqrt{\left(x_i-x_j\right)^2+\left(y_i-y_j\right)^2} \tag{1}$$

As shown in Fig. 1(b), 60 ($M\times N$) red dots represent risk reference points, which are positive integer coordinates in the cartesian coordinate system $\Theta(x,y)$. Through Eq. (1), the distance matrix between tanks $\mathscr{D}^1_{|\mathscr{T}|\times|\mathscr{T}|}$, $\mathscr{T}=\{\text{Tank 1,Tank 2}\}$, and the distance matrix between tanks and risk reference points $\mathscr{D}^2_{\boldsymbol{N}\times\boldsymbol{M}\times|\mathscr{T}|}$ can be obtained.

2.2.2. Accident consequence modeling

Common accident types within chemical tank farms include fires, explosions, and toxic gas releases [44,45]. Accident consequence models [44] such as the pool fire model, the jet fire model, the BLEVE explosion model, the VCE model, the Gaussian plume model, etc., can be used to calculate the radiation intensity, peak static overpressure, or gas concentration resulting from the corresponding accidents. As a result, the accident consequence matrices $\mathscr{I}^1=\left(I_{ij}\right)_{|\mathscr{T}|\times|\mathscr{T}|}$ and $\mathscr{I}^2=\left(I_{t,(x,y)}\right)_{\boldsymbol{N}\times\boldsymbol{M}\times|\mathscr{T}|}$ can be obtained, where $I_{i,j}$ is the radiation intensity or peak static overpressure received by Tank i from Tank j, $I_{t,(x,y)}$ is the radiation intensity, peak static overpressure or gas concentration received by location (x,y) from Tank t.

2.2.3. Domino escalation probability calculation

On the basis of accident consequence modeling results, the *Probit* model [45] is used for calculating domino escalation probability matrix $\mathscr{P}^{\boldsymbol{do}}=\left(\mathrm{P}^{\mathrm{do}}_{i,j}\right)_{|\mathscr{T}|\times|\mathscr{T}|}$, where $\mathrm{P}^{\mathrm{do}}_{i,j}$ is the domino escalation probability of tank i caused by tank j accident.

$$\mathrm{P}^{\mathrm{do}}_{i,j}=\frac{1}{\sqrt{2\pi}}\int_{-\infty}^{Y-5}e^{-\frac{x^2}{2}}dx \tag{2}$$

where the probit function Y of domino escalation probability is stated in the Appendix, Table C.1, which can be determined according to the equipment type & characteristics, accident type, and consequence intensity.

2.2.4. Personnel death probability calculation

Similarly, personnel death probability matrix $\mathscr{P}^{\boldsymbol{de}}=\left(\mathrm{P}^{\mathrm{de}}_{t,(x,y)}\right)_{\boldsymbol{N}\times\boldsymbol{M}\times|\mathscr{T}|}$ can be obtained by the *Probit* model [45], $\mathrm{P}^{\mathrm{de}}_{t,(x,y)}$ is the personnel death probability of location (x,y) caused by tank t accident.

$$\mathrm{P}^{\mathrm{de}}_{t,(x,y)}=\frac{1}{\sqrt{2\pi}}\int_{-\infty}^{Y-5}e^{-\frac{x^2}{2}}dx \tag{3}$$

where the probit function Y of personnel death probability is stated in the Appendix, Table D.1, which can be determined according to the accident type, consequence intensity, and personnel exposure time.

2.3. Risk superposition module

Following the Chinese Standard GB 36,894–2018 [50] and QRA framework [44,45], the risk value of any geographical location in the tank farm is determined by the individual risk, which can be defined as the product of accident probability and consequence. The accident probability is determined by the basic failure frequency and domino escalation probability of tanks. The accident consequence is measured by the personnel death probability. Thus, the risk value of $(x,y)\in\Theta$ can be calculated and superimposed as follows:

$$Risk(x,y)=\sum_{t\in\mathscr{T}}\mathrm{P}_{bf}\times\left[\mathrm{P}^{\mathrm{de}}_{t,(x,y)}+\sum_{j\in\mathscr{T}\,j\neq t}\left(\mathrm{P}^{\mathrm{do}}_{t,j}\times\mathrm{P}^{\mathrm{de}}_{j,(x,y)}\right)\right] \tag{4}$$

where $\mathrm{P}^{\mathrm{de}}_{t,(x,y)}$ represents the personnel death probability at point (x,y) caused by Tank t accident; $\mathrm{P}^{\mathrm{do}}_{t,j}$ is the domino escalation probability of Tank j caused by Tank t accident. In this work, the risk value at any point is determined by the cumulative risk from all tanks. The risk matrix $\mathscr{R}_{\boldsymbol{N}\times\boldsymbol{M}}$ can be obtained by calculating the risk values for all risk reference points.

2.4. High-risk area identification module

In practical applications, the risk matrix is relatively sparse, and interpolation methods can be used to obtain the overall regional risk distribution. In this project, the proposed risk program is implemented using MATLAB R2023a software. The built-in function *interp2*[1] is adopted for interpolation, *imagesc*[2] is adopted to draw the risk distribution map based on the risk matrix, and *contour*[3] is adopted to identify high-risk areas where the risk value is greater than the risk threshold μ.

3. Pareto-based optimization methodology

In this section, a pareto-based optimization methodology is proposed for chemical tank farm design, including a bi-objective optimization model and the corresponding model solving strategy.

3.1. Bi-objective optimization model

A bi-objective optimization model is defined for domino risk minimization and land resource utilization efficiency maximization. To be specific, the model decision variables are defined by the real-coded design parameter tuple $\mathscr{S}=\left\langle\mathbf{X}_{1\times|\mathscr{T}|},\mathbf{Y}_{1\times|\mathscr{T}|},\mathbf{D}_{1\times|\mathscr{T}|},\mathbf{H}_{1\times|\mathscr{T}|}\right\rangle$, where $\mathbf{X}_{1\times|\mathscr{T}|}$ is the abscissa vector of tanks, $\mathbf{Y}_{1\times|\mathscr{T}|}$ is the ordinate vector of tanks, $\mathbf{D}_{1\times|\mathscr{T}|}$ is the tank diameter vector, $\mathbf{H}_{1\times|\mathscr{T}|}$ is the tank height vector. The two model optimization objectives are defined as follows:

[1] https://www.mathworks.com/help/matlab/ref/interp2.html
[2] https://www.mathworks.com/help/matlab/ref/imagesc.html
[3] https://www.mathworks.com/help/matlab/ref/contour.html

Algorithm 2
Simulated annealing-based multi-objective particle swarm optimization.

Input: Instance Data; Swarm size N_P; Initial temperature T_0; Temperature damping rate γ
Output: Pareto-optimal Front ND_{set}
Initialization: $g = 1$
  Initial Swarm Construction: $\mathscr{S}_i(\mathrm{pos}_i^g, \mathrm{vel}_i^g, Z_1(\mathrm{pos}_i^g), Z_2(\mathrm{pos}_i^g)), i = 1,2,3,\ldots,N_P$
  Initial Global Non-dominated Set Construction: $ND_{set} \leftarrow \mathrm{ParetoRanking}(\{\mathscr{S}_1, \mathscr{S}_2, \ldots, \mathscr{S}_N\})$
  Initial Non-dominated Particle: $\Psi_i = \mathrm{pos}_i^g$
Iteration:
  While *stopping criterion not met* ***Do***
    For $i = 1$ *to* N_P ***Do***
      Particle Position Update: $\mathrm{pos}_i^{g+1} \leftarrow \mathrm{pos}_i^g + \mathrm{vel}_i^g$
      Particle Position Evaluation: $Z_1(\mathrm{pos}_i^g), Z_2(\mathrm{pos}_i^g)$
      If $\mathrm{pos}_i^{g+1} \succ \mathrm{pos}_i^g$ ***Do***
        Non-dominated Particle Update: $\Psi_i = \mathrm{pos}_i^{g+1}$
      End If
      If $\alpha < e^{-\frac{1}{T_0 \gamma^g}}$ ***Do***
        $\mathrm{pos}_{gb} \leftarrow \mathrm{RandomSelect}(\{\mathscr{S}_1, \mathscr{S}_2, \ldots, \mathscr{S}_N\})$
      Else If
        $\mathrm{pos}_{gb} \leftarrow \mathrm{RandomSelect}(ND_{set})$
      End If
      Particle Velocity Update: $\mathrm{vel}_i^{g+1} \leftarrow \omega \mathrm{vel}_i^g + c_1\, r_1 (\Psi_i - \mathrm{pos}_i^g) + c_2\, r_2 (\mathrm{pos}_{gb} - \mathrm{pos}_i^g)$
    End For
    Non-dominated Set Updtae: $ND_{set} \leftarrow \mathrm{ParetoRanking}(\{\mathscr{S}_1, \mathscr{S}_2, \ldots, \mathscr{S}_N\}, ND_{set})$
    $g = g + 1$
  End While

$$Maximize\ Z_1 = \frac{\sum_{t \in \mathscr{T}} V_t \rho_l}{S_F} \tag{5}$$

where the optimization objective function Z_1 focuses on maximizing the land resource utilization efficiency, S_F is the site area of the chemical tank farm, $[m^2]$, ρ_l is the density of the storage liquid, kg/m^3, $V_t = \frac{\pi D_t^2}{4} H_t$ is the volume of the tank $t \in \mathscr{T}$, $[\mathrm{m}^3]$. In this work, the land resource utilization efficiency is measured by the storage per unit area, $\left[\frac{\mathrm{kg}}{\mathrm{m}^2}\right]$.

$$Minimize\ Z_2 = contour(\mathscr{R}_{\boldsymbol{N}\times\boldsymbol{M}}, \Theta, \mu) \tag{6}$$

where the optimization objective function Z_2 focuses on minimizing the domino risk. In this work, the domino risk is measured by the area of high-risk zone, $[\mathrm{m}^2]$.

In practical applications, local chemical tank farm design regulations and standards can be satisfied by adding appropriate model constraints.

$$Model\ constraint\ 1:\ X_t + \frac{D_t}{2} \le Max.X, \forall t \in T \tag{7}$$

$$Model\ constraint\ 2:\ Y_t + \frac{D_t}{2} \le Max.Y, \forall t \in T \tag{8}$$

$$Model\ constraint\ 3:\ X_t - \frac{D_t}{2} \ge Min.X, \forall t \in T \tag{9}$$

$$Model\ constraint\ 4:\ Y_t - \frac{D_t}{2} \ge Min.Y, \forall t \in T \tag{10}$$

$$Model\ constraint\ 5:\ \frac{H_t}{D_t} \le Max.Ar, \forall t \in T \tag{11}$$

$$Model\ constraint\ 6:\ d_{ij} - \frac{D_i}{2} - \frac{D_j}{2} \ge Min.Fp, \forall i,j \in T \tag{12}$$

$$Model\ constraint\ 7:\ Max.D \ge D_t \ge Min.D, \forall t \in T \tag{13}$$

$$Model\ constraint\ 8:\ \mathrm{Max}.H \ge H_t \ge Min.H, \forall t \in T \tag{14}$$

where Max.X, Min.X, Max.Y, Min.Y form the tank design area boundary, model constraints 1 to 4 are used to ensure that tanks are not placed outside the tank design area boundary; Max.Ar represents the maximum allowable aspect ratio, for large-capacity tanks, the aspect ratio is generally not allowed to exceed 1.6 [51]; Min.Fp is the minimum allowable fire prevention distance between two tanks, model constraint 6 is used to ensure that the distance between any two tanks cannot be less than Min.Fp. As shown in the Appendix, Table E.1, the minimum allowable fire prevention distance, for instance in China, can be determined by the Chinese Standard GB50160–2008 [52]; model constraints 8 and 9 are tank dimension constraints.

3.2. Model solving strategy

The construction of the bi-objective optimization model is not sufficient for a realistic chemical tank farm design problem. Considering the real-coded model characteristics, the synergetic action mechanism of particle swarm optimization (PSO) has shown great performance in handling real-coded optimization problems [53]. However, due to the requirements of various policies, regulations and standards, the proposed bi-objective optimization model is associated with complex constraints, leading to the fragmentation of feasible solution space. Due to the vague boundary between the exploration and exploitation phases, PSO may easily fall into a local optimum. In addition, unlike single objective optimization problems, an MOP requires the optimization of multiple objectives at the same time.

Under this impetus, a well-designed simulated annealing-based multi-objective particle swarm optimization (SA-MOPSO) is therefore proposed for model solving. The general procedure of SA-MOPSO is shown in the pseudocode Algorithm 2. The proposed SA-MOPSO starts with a randomly generated particle swarm $\{\mathscr{S}_1, \mathscr{S}_2, \ldots, \mathscr{S}_N\}$. Each particle $\mathscr{S}_i, i = 1,2,3,\ldots,N_P$ is represented by its position pos_i^g, velocity vel_i^g and optimization objective values $Z_1(\mathrm{pos}_i^g), Z_2(\mathrm{pos}_i^g)$.

Given the multi-objective nature of chemical tank farm design problem, safety and economy related optimization preferences are required to be considered with the same importance [28,48,54]. Thus, the ***Pareto-dominance relationship*** [28,48,54] is adopted to discriminate particles in the swarm, and a set of Pareto optimal solutions should be obtained.

Definition. 1. **(*Pareto-dominance relationship*)** [28,48,54]: Suppose that $\mathscr{S}_i$ and $\mathscr{S}_j$ are two particles in the feasible solution space, $\mathscr{S}_i$ is not worse on all optimization objectives and better on at least one

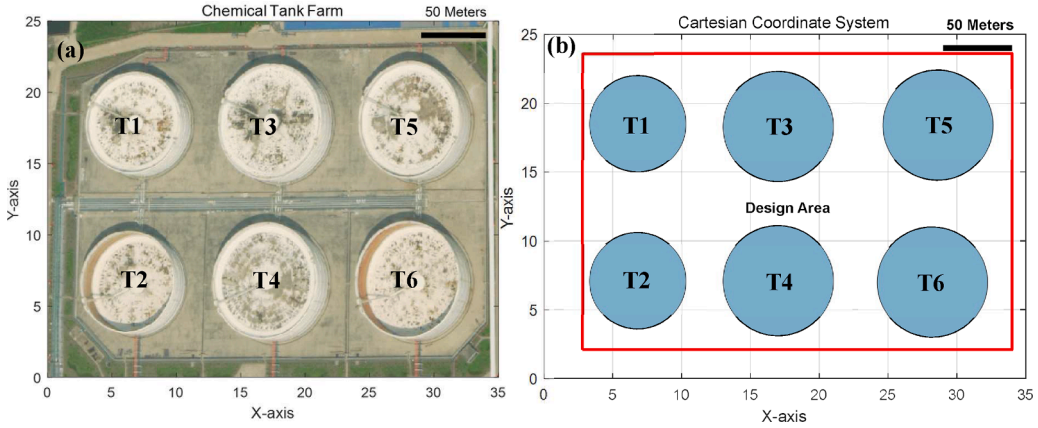

Fig. 2. Application scenario. (a). Chemical tank farm; (b) Cartesian coordinate system.

optimization objective than $\mathscr{S}_j$, we have $\mathscr{S}_i$ dominates $\mathscr{S}_j$, i.e. $\mathscr{S}_i \succ \mathscr{S}_j$. $\mathscr{S}_i$ is called a non-dominated particle or a pareto optimal solution if there are no other particles in the feasible solution space that can dominate $\mathscr{S}_i$. The set of non-dominated particles is called the Pareto-optimal set (POS) or Pareto-optimal front (POF).

A synergetic action among the particles is adopted to approach the true POF [53]. During the process of iteration, the particle positions and velocities are constantly updated.

$$\mathrm{pos}_i^{g+1} \leftarrow \mathrm{pos}_i^g + \mathrm{vel}_i^g \tag{15}$$

$$vel_i^{g+1} \leftarrow \omega vel_i^g + c_1\, r_1 \left(\Psi_i - pos_i^g\right) + c_2\, r_2 \left(pos_{gb} - pos_i^g\right) \tag{16}$$

where pos_i^g is the position of particle i at iteration g; vel_i^g is the velocity of particle i at iteration g; c_1 and c_2 are two learning coefficients; r_1 and r_2 are two random numbers; $\omega = \omega_{max} - \frac{(\omega_{max}-\omega_{min})g}{G_{max}}$ is an adaptive inertia weight decreasing with the iteration process [53]. Ψ_i is the non-dominated position of particle i. pos_{gb} is a non-dominated or dominated particle randomly selected from the swarm $\{\mathscr{S}_1, \mathscr{S}_2, \ldots, \mathscr{S}_N\}$ or the non-dominated set ND_{set}. Simulated annealing [41] introduces a jumping mechanism in the iteration process, allowing for the probabilistic acceptance ($\alpha < e^{-\frac{1}{T_0 \gamma^g}}$) of dominated particles as reference positions. Through the simulated annealing process, SA-MOPSO can explore a wider feasible solution space and avoid falling into local optimum caused by complex constraints.

4. Case study

A case study is given to demonstrate the proposed methodology. As shown in Fig. 2(a), a chemical tank farm is offered as a case-study. The scale factor Δ is set to be 10 m. As shown in Fig. 2(b), a cartesian coordinate system $\Theta(x, y), x \in [0, 35], y \in [0, 25]$ is constructed.

Six floating roof diesel tanks are located in this chemical tank farm. The diameter of T1 and T2 is 70 m and the tank height is 35 m. The diameter of T1, T2, T3, T4 is 80 m and the tank height is 40 m. The rectangular region enclosed by the red line in Fig. 2(b) is considered as the design area. Correspondingly, the tank design area boundary is Max.$X = 34.0$, Min.$X = 2.8$, Max.$Y = 23.6$, Min.$Y = 2.1$. The site area of the chemical tank farm $S_F = 6.708\mathrm{e}+04\mathrm{m}^2$. Furthermore, diesel is a flammable, low volatility liquid. The potential accident considered is a pool fire. To facilitate comparative analysis, a fixed aspect ratio of 0.5 is adopted. The minimum allowable tank diameter Min.D is set to be 40 m. The basic failure frequency of tanks is set to be $1\mathrm{e}-04$. According to the Appendix, Table A.1, the risk threshold μ is set to be $3\mathrm{e}-05$.

4.1. Quantitative risk assessment

As shown in Fig. 3(a), the proposed S-QRA procedure is adopted to obtain the individual risk distribution for the case-study considered. The assessment results indicate a strong correlation between the distribution of individual risk and the storage tank locations. The individual risk values for risk reference points near the tanks are significantly higher than those for reference points located at the perimeter. Furthermore,

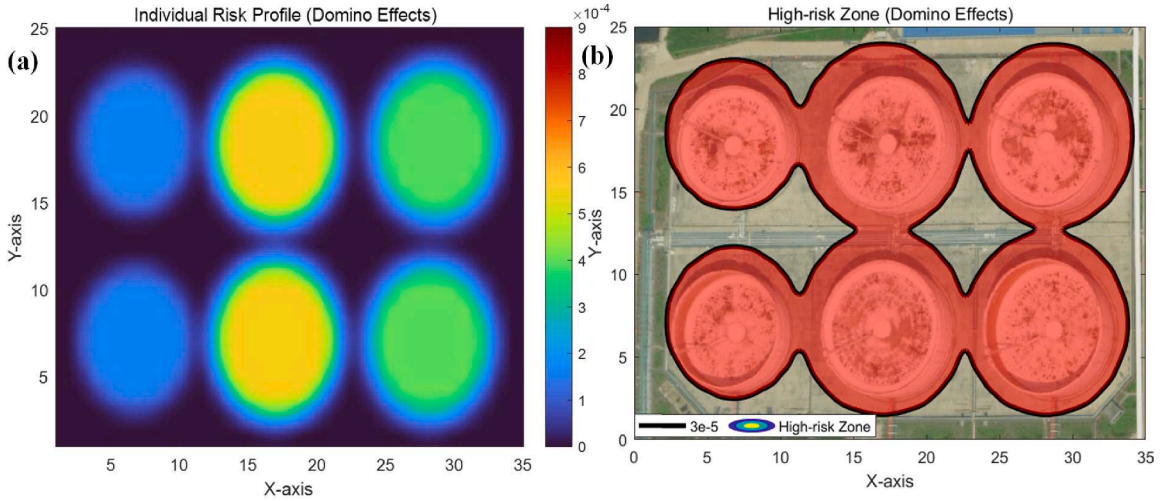

Fig. 3. Quantitative risk assessment results with the consideration of domino effects. (a). Individual risk profile; (b) High-risk zone.

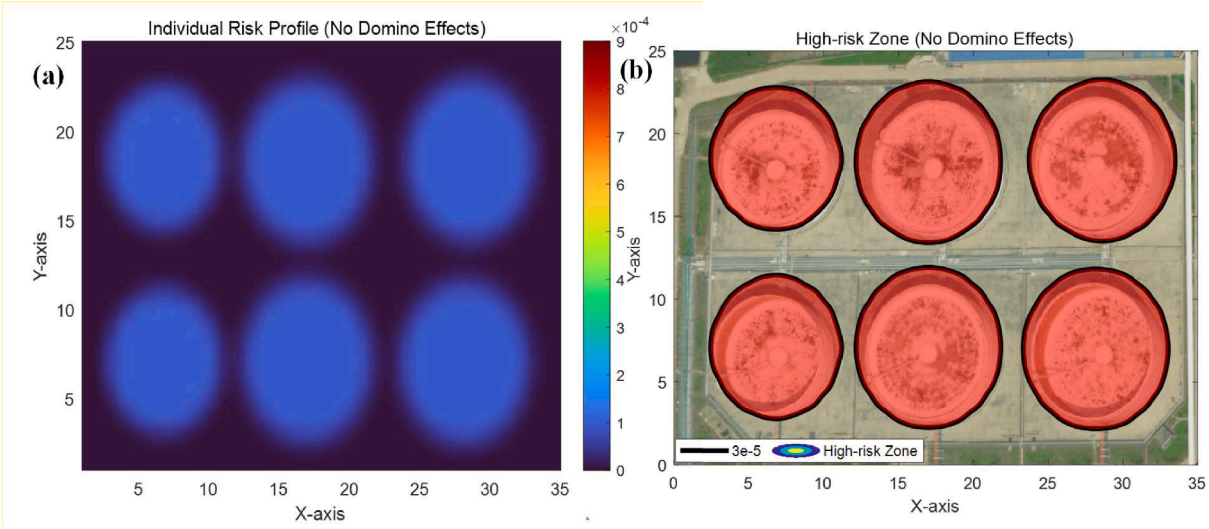

Fig. 4. Quantitative Risk Assessment Results without the Consideration of Domino Effects. (a). Individual Risk Profile; (b) High-risk Zone.

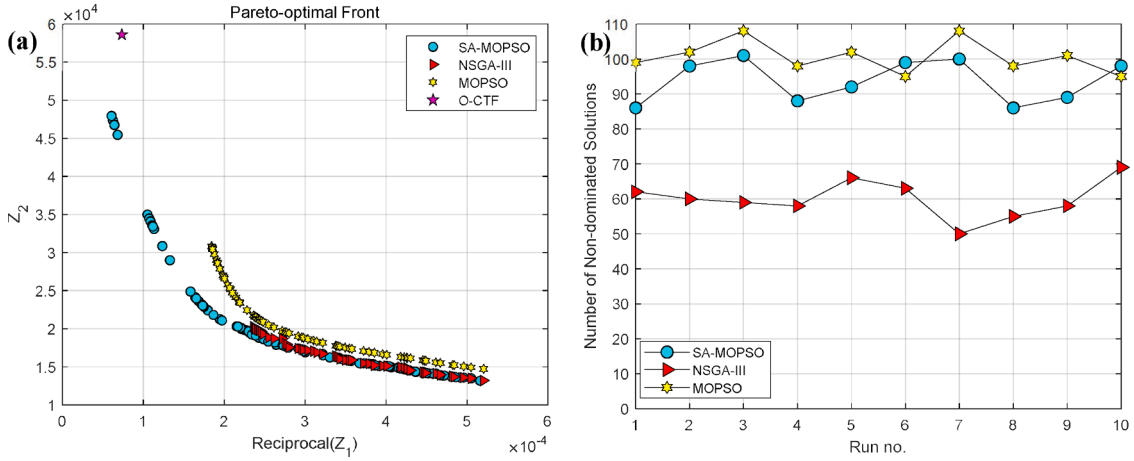

Fig. 5. Algorithm Performance Analysis. (a). Pareto-optimal Front; (b) Number of Non-dominated Solutions.

the individual risk values in the central region of the chemical tank farm are significantly higher. Additionally, as shown in Fig. 3(b), due to the superposition of individual risk, the risk reference points between T3 and T4, as well as between T5 and T6, are also located within the high-risk zone. The risk reference points between T1 and T2 are not located in high-risk zone. This is because the diameter of T1 and T2 is smaller and the fire prevention distance between T1 and T2 is larger. However, this also means that the volume of T1 and T2 is smaller. According to the bi-objective optimization model, the two model optimization objectives are: $Z_1 = 1.361e + 04$ kg/m^2 and $Z_2 = 5.862e + 04$m^2.

Further, to analyze the impact of the domino effects on the risk distribution, the QRA results without the consideration of domino effects are shown in Fig. 4. As shown in Fig. 4(a), the individual risk values in the chemical tank farm are relatively low, while domino effects are ignored. Furthermore, as shown in Fig. 4(b), the risk reference points between tanks are not located within the high-risk zone. Correspondingly, the two model optimization objectives are: $Z_1 = 1.361e + 04$ kg /m^2 and $Z_2 = 4.114e + 04$m^2. Comparative analysis indicates that domino effects significantly increase the individual risk values, leading to a larger high-risk zone.

4.2. Algorithm performance analysis

The algorithm performance is measured by the diversity and the convergence of the obtained POF. To demonstrate the advantages of the proposed algorithm, SA-MOPSO is compared with two classical multi-objective evolutionary algorithms, i.e., multi-objective particle swarm optimization (MOPSO) and non-dominated sorting genetic algorithm III (NSGA-III) [55]. MOPSO adopts the same position and velocity update strategy as SA-MOPSO but without the simulated annealing-based jumping mechanism. The comparison between SA-MOPSO and MOPSO can be regarded as the ablation analysis. NSGA-III adopts the real-coded genetic evolution mechanism for model solving, which is different from the synergetic action mechanism of PSO.

After some preliminary pre-simulations, the swarm size N_P is set to be 100 and the maximum iteration number is set to 500. The stochasticity of evolutionary algorithms may lead the instability of algorithm performance [41,55]. To avoid any loss of generality, each of the three algorithms is independently executed ten times [54,56].

For each algorithm, the non-dominated solutions obtained from ten independent runs are integrated to form the final POF. As shown in Fig. 5 (a), the final POFs obtained by three algorithms exhibit distinct convergence and diversity. Among the three algorithms, MOPSO exhibits the poorest convergence. The complex model constraints partition the feasible solution space, making MOPSO highly susceptible to falling into the local optimum, thus deteriorating its convergence. The simulated annealing-based jumping mechanism provides SA-MOPSO with a dynamic probability of accepting dominated solutions, effectively

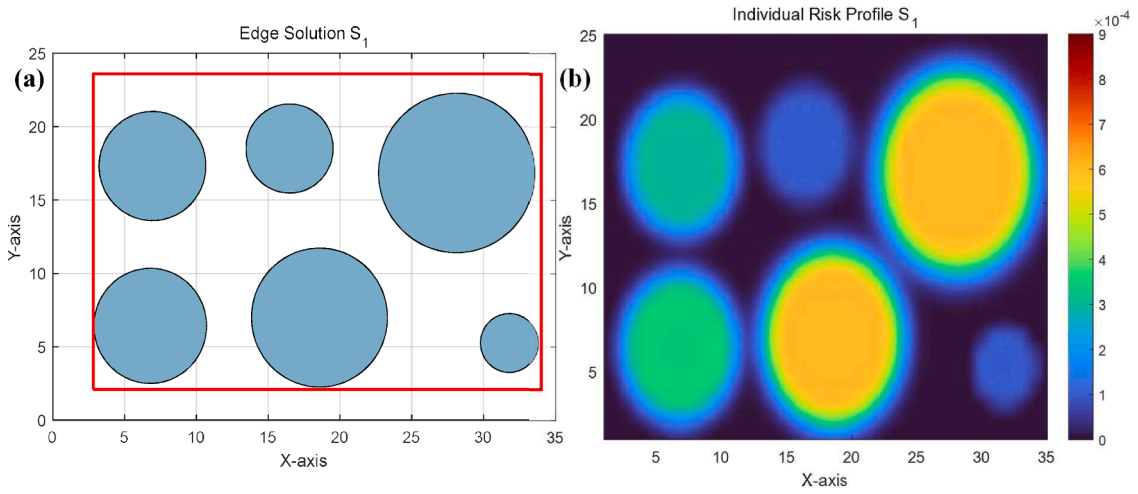

Fig. 6. Detailed Solution Analysis. (a) Design Solution $\mathscr{S}_1$; (b) Individual Risk Profile $\mathscr{S}_1$.

preventing the local optimum and improving the algorithm convergence. The temperature gradually decreases with the iteration process, thereby adjusting the acceptance probability and effectively regulating the exploration and exploitation phases of SA-MOPSO [53]. The purple pentagon in Fig. 5(a) represents the objective function values of the original chemical tank farm. It can be observed that the design of the original chemical tank farm is not Pareto optimal. The proposed methodology can obtain a set of pareto-optimal design solutions that outperform the original design in both optimization objectives.

Due to the segmentation of the feasible solution space, all the POFs are non-continuous. However, compared to SA-MOPSO and MOPSO, the POF obtained by NSGA-III appears to miss more non-dominated solutions. As shown in Fig. 5(b), the number of non-dominated solutions obtained by NSGA-III is significantly lower than that of SA-MOPSO and MOPSO. For a real-number encoding problem, the PSO particle update strategy is more efficient and can explore a wider feasible solution space.

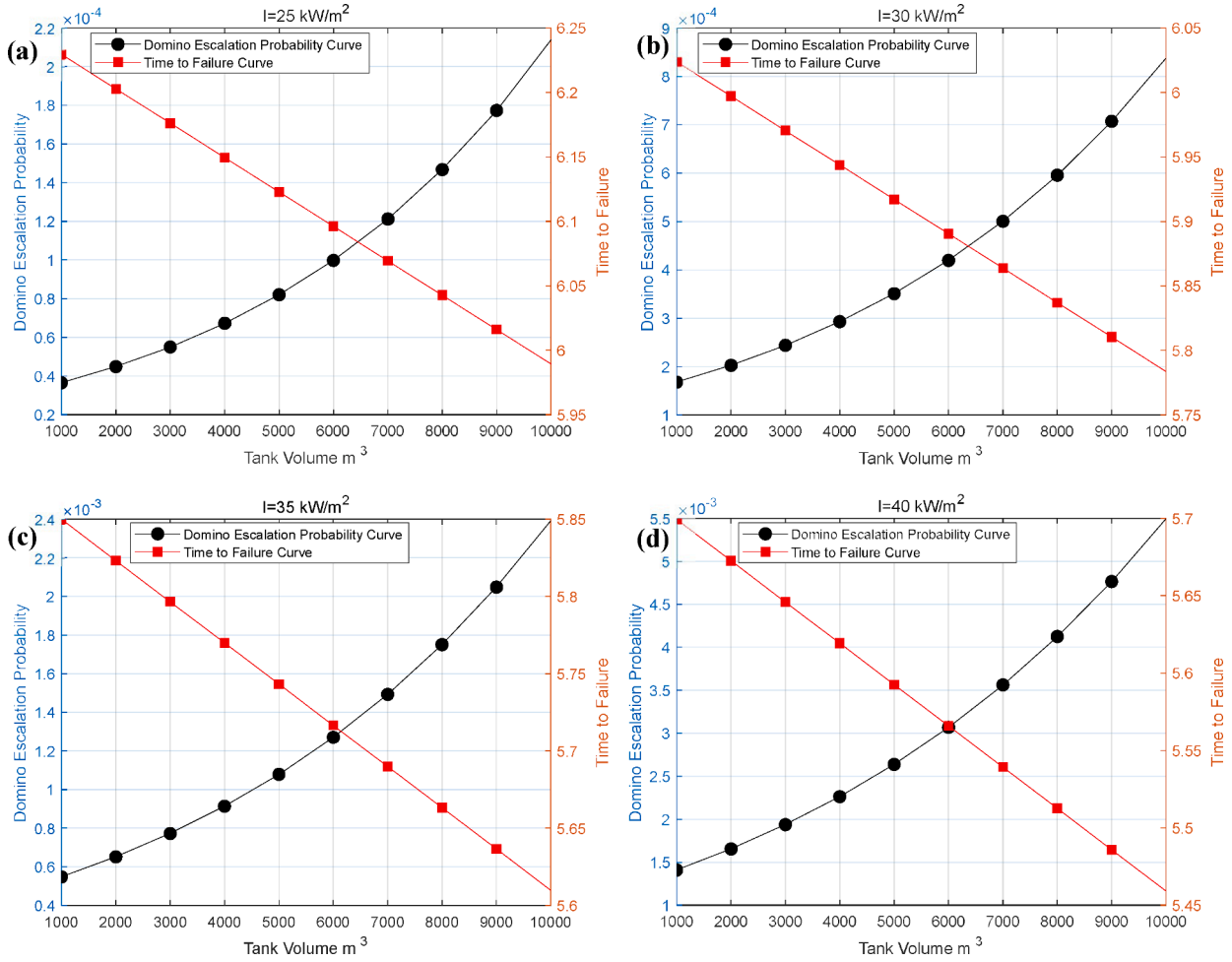

Fig. 7. Comparative Analysis of Domino Escalation Probability. (a) $I = 25$ kW·m^{-2}; (b) $I = 30$ kW·m^{-2}; (c) $I = 35$ kW·m^{-2}; (d) $I = 40$ kW·m^{-2}.

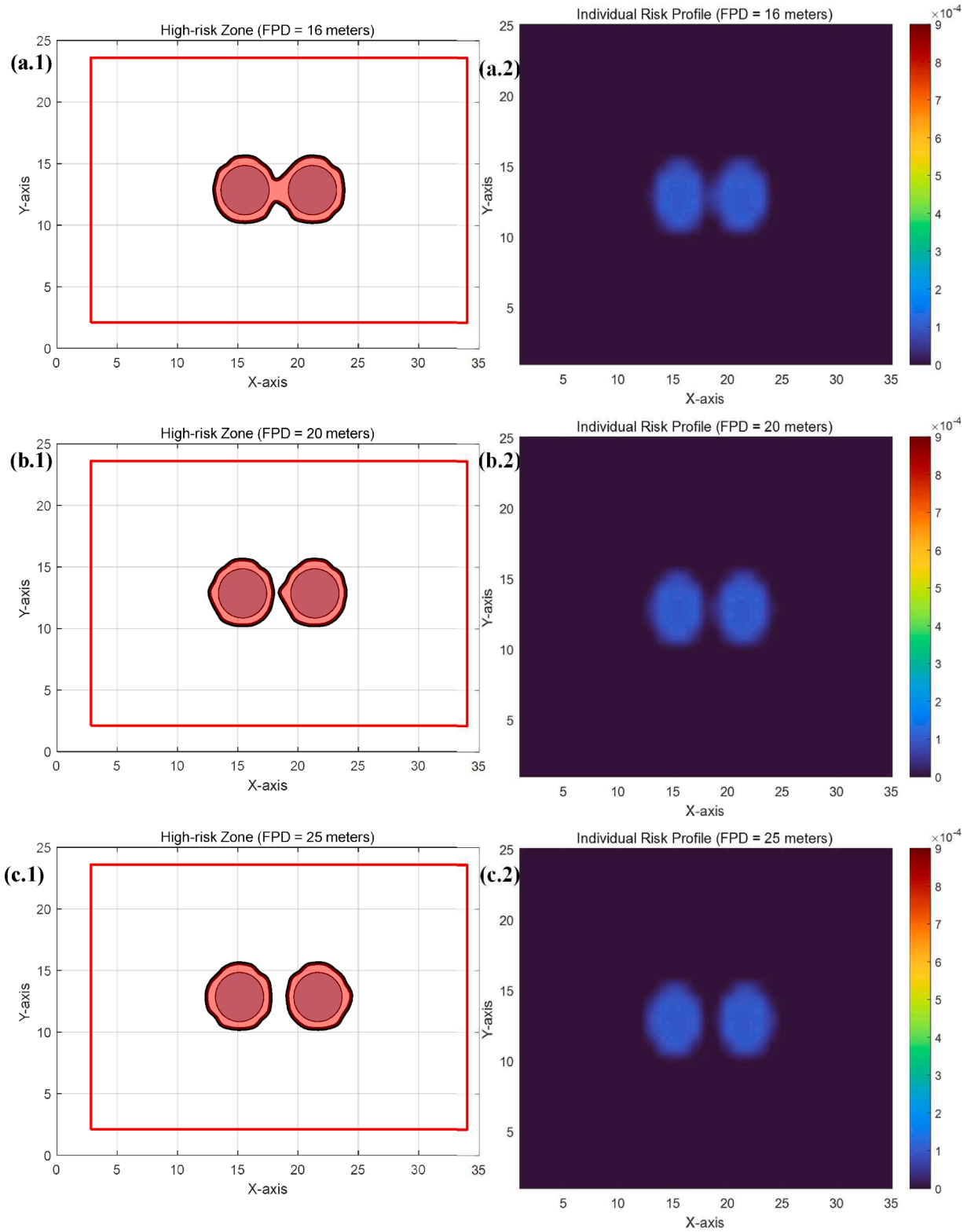

Fig. 8. Comparative Analysis of High-risk Zone. (a) *FPD* = 16 m; (b) *FPD* = 20 m; (c) *FPD* = 25 m.

This indicates that the diversity of the POFs obtained by SA-MOPSO and MOPSO are superior to that of NSGA-III.

4.3. Detailed solution analysis

After ten independent executions, SA-MOPSO obtained 100 pareto-optimal solutions. In this section, an edge solution $\mathscr{S}_1$ is extracted from the 100 pareto-optimal solutions, which is preferred by optimization objective Z_1. $\mathscr{S}_0$ is denoted as the original chemical tank farm (shown in Fig. 2). For original solution $\mathscr{S}_0$, the two optimization objectives $Z_1(\mathscr{S}_0) = 1.361\text{e}+04$ kg/m^2 and $Z_2(\mathscr{S}_0) = 5.862\text{e}+04$m^2. As shown in Fig. 6(a) and (b), for edge solution $\mathscr{S}_1$, the two optimization

objectives $Z_1(\mathscr{S}_1) = 1.647e+04$ kg/m^2 and $Z_2(\mathscr{S}_1) = 4.794e+04$m^2. Since $Z_1(\mathscr{S}_1) > Z_1(\mathscr{S}_0)$ and $Z_2(\mathscr{S}_1) < Z_2(\mathscr{S}_0)$, $\mathscr{S}_1$ is better on all optimization objectives than $\mathscr{S}_0$. According to the *Definition.* 1, we have $\mathscr{S}_1$ dominates $\mathscr{S}_0$, i.e., $\mathscr{S}_1 \succ \mathscr{S}_0$.

Compared to the original chemical tank farm, edge solution $\mathscr{S}_1$ employs a diversified chemical tank farm design strategy, which involves constructing tanks of different sizes within the design area. This simultaneously enhances land resource utilization efficiency and reduces the domino effect risk.

5. Discussion

From the perspective of economy, design preference focuses on how to use limited resources to achieve higher level industrial functions. From the perspective of safety, design preference focuses on how to eliminate, prevent and mitigate potential hazards. In this section, conflicting nature between domino risk minimization and land resource utilization efficiency maximization is discussed.

As shown in Fig. 7, the domino escalation probability and the corresponding time to failure (*ttf*) of different volume tanks exposed to thermal radiation intensities of 25 kW·m^{-2}, 30 kW·m^{-2}, 35 kW·m^{-2}, 40 kW·m^{-2} are analyzed. Comparative analysis results indicate that under the same thermal radiation intensity, large-scale tanks have a shorter *ttf*, resulting in a higher domino escalation probability. However, large-scale tanks can often store a greater quantity of hazardous chemicals, thereby improving land resource utilization efficiency.

Furthermore, the impact of the fire prevention distance *FPD* on domino risk distribution is analyzed. Suppose that a chemical tank farm is equipped with two diesel floating roof tanks with a diameter of 40 m and a height of 20 m, *FPD* between tanks is set to be 16 m, 20 m, and 25 m, respectively.

The corresponding high-risk zones are shown in Fig. 8. To be specific, for the scenario with $FPD = 16$ m, the two optimization objectives are $Z_1(FPD = 16\text{ m}) = 6.370e+02$ kg/m^2 and $Z_2(FPD = 16\text{ m}) = 4.458e+03$ m^2. For the scenario with $FPD = 20$ m, the two optimization objectives are $Z_1(FPD = 20\text{ m}) = 6.370e+02$ kg/m^2 and $Z_2(FPD = 20\text{ m}) = 4.369e+03$ m^2. For the scenario with $FPD = 25$ m, the two optimization objectives are $Z_1(FPD = 25\text{ m}) = 6.370e+02$ kg/m^2 and $Z_2(FPD = 25\text{ m}) = 4.409e+03$ m^2.

Comparative analysis results indicate that the increase of *FPD* can effectively reduce the domino risk values. However, increasing *FPD* implies the need for more land resources to meet storage requirements, reducing land resource utilization efficiency. The conflicting nature of safety and economy is the key to form a pareto-optimal front.

6. Conclusion

In this work, a pareto-based chemical tank farm design methodology is proposed for domino risk minimization and land resource utilization efficiency maximization. The objective of this work is to provide an advanced inherent safety design tool that can achieve trade-off between safety and economy. To be specific, a simplified quantitative domino risk assessment procedure is developed within a grid-based Cartesian coordinate system, which links the design parameters and domino risk values. A bi-objective optimization model is developed for problem formulation and a well-designed simulated annealing-based multi-objective particle swarm optimization is proposed for model solving. The methodology advantages are verified on a chemical tank farm with six floating roof diesel tanks.

Risk analysis results indicate that domino effects significantly increase the individual risk values, leading to a larger high-risk zone. The regional risk distribution is closely related to the chemical tank farm design parameters.

The performance of simulated annealing-based multi-objective particle swarm optimization (SA-MOPSO) is compared with multi-objective particle swarm optimization (MOPSO) and non-dominated sorting genetic algorithm III (NSGA-III). Comparative analysis results indicate that the proposed SA-MOPSO outperforms MOPSO and NSGA-III. The simulated annealing-based jumping mechanism can effectively avoid the local optimum, which makes SA-MOPSO easier to obtain the Pareto-optimal front with great convergence and diversity. Compared to the original chemical tank farm, the proposed methodology can provide safer and more cost-effective design solutions through diversified chemical tank farm design strategy.

Conflicting nature between domino risk minimization and land resource utilization efficiency maximization was discussed. The pareto-based optimization methodology can obtain a set of pareto-optimal solutions to meet different design preferences, which provides a new and comprehensive perspective for the design of chemical tank farms.

CRediT authorship contribution statement

Jinkun Men: Writing – review & editing, Writing – original draft, Validation, Software, Methodology, Investigation, Formal analysis, Data curation, Conceptualization. **Guohua Chen:** . **Genserik Reniers:** Writing – review & editing, Conceptualization.

Declaration of competing interest

The authors declare the following financial interests/personal relationships which may be considered as potential competing interests:

Guohua Chen reports financial support was provided by South China University of Technology.

Data availability

Data will be made available on request.

Acknowledgements

This study was supported by the National Natural Science Foundation of China (22078109), the Key-Area Research and Development Program of Guangdong Province (2019B111102001), the China Scholarship Council (202206150061).

Appendix

A. Individual risk benchmark

According to the Chinese Standard [50], the individual risk borne by the protected targets around production installations and storage facilities for hazardous chemicals must not exceed the individual risk benchmark specified in Table A. 1.

Table A.1
Individual risk benchmark for different protected targets [50].

Protected Targets	Individual Risk Benchmark (per year)	
	Newly constructed, retrofitted, or expanded production installations and storage facilities.	Operational production installations and storage facilities.
Highly sensitive protected targets* Important protected targets** First class protected targets***	$\leq 3e-07$	$\leq 3e-06$
Second class protected targets[3]	$\leq 3e-06$	$\leq 1e-05$
Third class protected targets[3]	$\leq 1e-05$	$\leq 3e-05$

* Cultural facilities, educational facilities, healthcare establishments, social welfare facilities, etc.
** Public library exhibition facilities, cultural heritage conservation sites, religious venues, urban rail transit system, military installations, diplomatic offices, etc.
*** Other general protected targets.

B. *Basic failure frequency*

Table B.1
Basic failure frequency of chemical storage tanks [57].

Tank Type	Failure Frequency (per year)			
	Minor Leakage	Medium Leakage	Major Leakage	Collapse
Atmospheric Tanks	$4e-05$	$1e-04$	$1e-05$	$2e-05$
Pressurized Tanks	$4e-05$	$1e-04$	$1e-05$	$6e-06$

C. *C. Domino escalation probability calculation*

Thermal radiation, blast waves, and fragments generated by fires and explosions may impose severe damage on adjacent units, leading to the so-called domino effects [18,19,45]. As mentioned by [45], the term "domino effect" is regarded as "an accident in which a primary event propagates to nearby equipment, triggering one or more secondary events resulting in overall sequences more severe than those of the primary event." As shown in Table C.1, the *Probit* model is widely used for calculating domino escalation probability.

$$P = \frac{1}{\sqrt{2\pi}} \int_{-\infty}^{Y-5} e^{-\frac{x^2}{2}} dx \tag{C.1}$$

Table C.1
Probit models for domino escalation probability* [45].

Escalation Vector	Type	Probit Model
Fire Radiation	Atmospheric vertical cylindrical vessels	$Y = 12.54 - 1.847\ln_1(ttf)$ $\ln_1(ttf) = -1.128\ln(I) - 2.667 \times 10^{-5}V + 9.877$
	Pressurized horizontal cylindrical vessels	$Y = 12.54 - 1.847\ln_2(ttf)$ $\ln_2(ttf) = -0.947\ln(I) + 8.835V^{0.032}$
Explosion Overpressure	Atmospheric	$Y = -18.96 - 2.44\ln(P_s)$
	Pressurized	$Y = -42.44 + 4.33\ln(P_s)$
	Elongated	$Y = -28.07 + 3.16\ln(P_s)$
	Auxiliary	$Y = -17.79 + 2.18\ln(P_s)$

* ttf: time to failure (s); I: radiation intensity (kW·m^{-2}); V: Vessel volume (m^2); P_s: peak static overpressure on the target equipment (kPa).

D. *Personnel death probability calculation*

Table D.1
Probit models for personnel death probability* [45].

Injure Factors	Probit Model
Fire Radiation	$Y = -14.9 - 1.847\ln(6 \times 10^{-3} I^{1.33} t_e)$
Explosion Overpressure	$Y = 5.13 - 1.37\ln(P_s)$
Chlorine release	$Y = -10.1 - 1.11\ln(C^{1.65} t_e)$
Ammonia Release	$Y = -9.82 - 0.71\ln(C^2 t_e)$

* C: toxic concentration (ppm); t_e: exposure time (min).

E. E. Fire prevention distance

According to the Chinese Standard [52], in a chemical tank farm, the minimum allowable fire prevention distance between two tanks is shown in Table E.1.

Table E.1
The minimum allowable fire prevention distance* [52].

Content Type	Tank Type			
	Fixed Roof Tank		Floating Tank	Horizontal Tank
	$\leq 1000m^3$	$> 1000m^3$		
A_2, B_1, B_2	$0.75D$	$0.6D$	$0.4D$	$0.8m$
C_1	$0.4D$			
C_2	$2m$	$5m$		

* D is the diameter of the larger of the two adjacent tanks; A_2 : flammable liquid with a flash point less than 28 °C and a vapor pressure (15 °C) less than 0.1 MPa; B_1 : flammable liquid with a flash point 28 to 45 °C; B_2 : flammable liquid with a flash point 45 to 60 °C; C_1 : flammable liquid with a flash point 60 to 120 °C; C_2 : flammable liquid with a flash point more than 120 °C.

References

[1] Khakzad N, Khan F, Amyotte P. Safety analysis in process facilities: comparison of fault tree and Bayesian network approaches. Reliab Eng Syst Saf 2011;96:925–32.
[2] He G, Boas IJC, Mol APJ, Lu Y. What drives public acceptance of chemical industrial park policy and project in China? Res, Conserv Recycl 2018;138:1–12.
[3] Men J, Chen G, Zeng T. Multi-hazard coupling effects in chemical process industry—part I: preliminaries and mechanism. IEEE Syst J 2023;17:1626–36.
[4] Men J, Chen G, Zeng T. Multi-hazard coupling effects in chemical process industry—part II: research advances and future perspectives on methodologies. IEEE Syst J 2023;17:1637–47.
[5] Iaiani M, Tugnoli A, Cozzani V. Identification of reference scenarios for security attacks to the process industry. Process Safety Environ Protect 2022;161:334–56.
[6] Reniers G, Khakzad N, Van GPieter. Security risk assessment in the chemical and process industry. Berlin, Boston: De Gruyter; 2018.
[7] Necci A, Cozzani V, Spadoni G, Khan F. Assessment of domino effect: state of the art and research Needs. Reliab Eng Syst Saf 2015;143:3–18.
[8] Wu X, Huang H, Xie J, Lu M, Wang S, Li W, Huang Y, Yu W, Sun X. A novel dynamic risk assessment method for the petrochemical industry using bow-tie analysis and Bayesian network analysis method based on the methodological framework of ARAMIS project. Reliab Eng Syst Saf 2023;237:109397.
[9] Men J, Chen G, Reniers G, Wu Y, Huang H. Experimental and numerical study on earthquake-fire coupling failure mechanism of steel cylindrical tanks. Reliab Eng Syst Saf 2024;245:110016.
[10] Willey RJ. West fertilizer company fire and explosion: a summary of the U.S. chemical safety and hazard investigation board report. J Loss Prev Process Ind 2017;49:132–8.
[11] Zhang N, Shen S-L, Zhou A-N, Chen J. A brief report on the March 21, 2019 explosions at a chemical factory in Xiangshui, China. Process Safety Progress 2019;38:e12060.
[12] Sivaraman S, Varadharajan S. Investigative consequence analysis: a case study research of beirut explosion accident. J Loss Prev Process Ind 2021;69:104387.
[13] Park S, Xu S, Rogers W, Pasman H, El-Halwagi MM. Incorporating inherent safety during the conceptual process design stage: a literature review. J Loss Prev Process Ind 2020;63:104040.
[14] Logan TM, Aven T, Guikema SD, Flage R. Risk science offers an integrated approach to resilience. Nat Sustain 2022;5:741–8.
[15] He Z, Shen K, Lan M, Weng W. The effects of dynamic multi-hazard risk assessment on evacuation strategies in chemical accidents. Reliab Eng Syst Saf 2024;246:110044.
[16] Bai M, Qi M, Shu C-M, Reniers G, Khan F, Chen C, Liu Y. Why do major chemical accidents still happen in China: analysis from a process safety management perspective. Process Safety Environ Protect 2023;176:411–20.
[17] Ricci F, Moreno VCasson, Cozzani V. A comprehensive analysis of the occurrence of Natech events in the process industry. Process Safety Environ Protect 2021;147:703–13.
[18] Cozzani V, Tugnoli A, Salzano E. Prevention of domino effect: from active and passive strategies to inherently safer design. J Hazard Mater 2007;139:209–19.
[19] Men J, Chen G, Yang Y, Reniers G. An event-driven probabilistic methodology for modeling the spatial-temporal evolution of natural hazard-induced domino chain in chemical industrial parks. Reliab Eng Syst Saf 2022;226:108723.
[20] Reniers GLL, Dullaert W, Ale BJM, Soudan K. Developing an external domino accident prevention framework: hazwim. J Loss Prev Process Ind 2005;18:127–38.
[21] Jia M, Chen G, Reniers G. Equipment vulnerability assessment (EVA) and pre-control of domino effects using a five-level hierarchical framework (FLHF). J Loss Prev Process Ind 2017;48:260–9.
[22] Zeng T, Chen G, Reniers G, Men J. Developing a barrier management framework for dealing with Natech domino effects and increasing chemical cluster resilience. Process Safety Environ Protection 2022;168:778–91.
[23] Yang Y, Chen G, Zhao Y. A quantitative framework for propagation paths of natech domino effects in chemical industrial parks: part II—risk assessment and mitigation system. Sustainability 2023.
[24] Tugnoli A, Cozzani V, Di Padova A, Barbaresi T, Tallone F. Mitigation of fire damage and escalation by fireproofing: a risk-based strategy. Reliab Eng Syst Saf 2012;105:25–35.
[25] Zheng Y-J, Chen S-Y, Xue Y, Xue J-Y. A pythagorean-type fuzzy deep denoising autoencoder for industrial accident early warning. IEEE Trans Fuzzy Syst 2017;25:1561–75.
[26] Villa V, Reniers GLL, Paltrinieri N, Cozzani V. Development of an economic model for the allocation of preventive security measures against environmental and ecological terrorism in chemical facilities. Process Safety Environ Protect 2017;109:311–39.
[27] Chen C, Reniers G, Khakzad N. Integrating safety and security resources to protect chemical industrial parks from man-made domino effects: a dynamic graph approach. Reliab Eng Syst Saf 2019;191:106470.
[28] Men J, Jiang P, Zheng S, Kong Y, Zhao Y, Sheng G, Su N, Zheng S. A multi-objective emergency rescue facilities location model for catastrophic interlocking chemical accidents in chemical parks. IEEE Trans Intell Transport Syst 2020;21:4749–61.
[29] Wang R, Wang Y, Gundersen T, Wu Y, Feng X, Liu M. A multi-objective optimization method for industrial park layout design: the trade-off between economy and safety. Chem Eng Sci 2021;235:116471.
[30] Zhu J, Liu Z, Cao Z, Han X, Hao L, Wei H. Development of a general inherent safety assessment tool at early design stage of chemical process. Process Safety Environ Protect 2022;167:356–67.
[31] Zhou J, Reniers G. Petri-net based cooperation modeling and time analysis of emergency response in the context of domino effect prevention in process industries. Reliab Eng Syst Saf 2022;223:108505.
[32] Guo X, Ding L, Ji J, Cozzani V. A cost-effective optimization model of safety investment allocation for risk reduction of domino effects. Reliab Eng Syst Saf 2022;225:108584.
[33] Zhou J, Reniers G, Cozzani V. A Petri-net approach for firefighting force allocation analysis of fire emergency response with backups. Reliab Eng Syst Saf 2023;229:108847.
[34] Khakzad N. A goal programming approach to multi-objective optimization of firefighting strategies in the event of domino effects. Reliab Eng Syst Saf 2023;239:109523.
[35] Yuan S, Reniers G, Yang M. Dynamic-risk-informed safety barrier management: an application to cost-effective barrier optimization based on data from multiple sources. J Loss Prev Process Ind 2023;83:105034.
[36] He Z, Shen K, Lan M, Weng W. An evacuation path planning method for multi-hazard accidents in chemical industries based on risk perception. Reliab Eng Syst Saf 2024;244:109912.
[37] Gao X, Abdul Raman AA, Hizaddin HF, Bello MM, Buthiyappan A. Review on the Inherently Safer Design for chemical processes: past, present and future. J Clean Prod 2021;305:127154.
[38] Men J, Chen G, Reniers G. Time-dependent earthquake-fire coupling fragility analysis under limited prior knowledge: a perspective from type-2 fuzzy probability. Process Safety Environ Protect 2024;183:274–92.
[39] Amyotte PR, Khan FI. The role of inherently safer design in process safety. Can J Chem Eng 2021;99:853–71.
[40] Yazdi M, Nedjati A, Zarei E, Adumene S, Abbassi R, Khan F. Chapter thirteen - domino effect risk management: decision making methods. In: Khan F, Cozzani V, Reniers G, editors. Methods in chemical process safety. Elsevier; 2021. p. 421–60.
[41] Men J, Jiang P, Xu H. A chance constrained programming approach for HazMat capacitated vehicle routing problem in Type-2 fuzzy environment. J Clean Prod 2019;237:117754.
[42] Khan F, Rathnayaka S, Ahmed S. Methods and models in process safety and risk management: past, present and future. Process Safety Environ Protect 2015;98:116–47.

[43] Khan FI, Abbasi SA. Techniques and methodologies for risk analysis in chemical process industries. J Loss Prev Process Ind 1998;11:261–77.
[44] CCPS. Guidelines for chemical process quantitative risk analysis. 2nd Edition. US: New York: American Institute of Chemical Engineers; 2000.
[45] Cozzani V, Gubinelli G, Antonioni G, Spadoni G, Zanelli S. The assessment of risk caused by domino effect in quantitative area risk analysis. J Hazard Mater 2005; 127:14–30.
[46] Liu X, Wang C, Yin Z, An X, Meng H. Risk-informed multi-objective decision-making of emergency schemes optimization. Reliab Eng Syst Saf 2024;245:109979.
[47] Di Maio F, Marchetti S, Zio E. Robust multi-objective optimization of safety barriers performance parameters for NaTech scenarios risk assessment and management. Reliab Eng Syst Saf 2023;235:109245.
[48] Men J, Chen G, Zhou L, Chen P. A pareto-based multi-objective network design approach for mitigating the risk of hazardous materials transportation. Process Safety Environ Protect 2022;161:860–75.
[49] Reniers G. Operational safety economics: a practical approach focused on the chemical and process industries. John Wiley & Sons, Ltd; 2016.
[50] GB36894-2018, Risk criteria for hazardous chemicals production unit and storage installations, in, State Administration of Market Regulation, Beijing, 2018.
[51] GB50341-2014, Code for design of vertical cylindrical welded steel oil tanks, in, Ministry of Housing and Urban-Rural Development, Beijing, 2014.
[52] GB50160-2008, Standard for fire prevention design of petrochemical enterprise, in, Ministry of Housing and Urban-Rural Development, Beijing, 2018.
[53] Men J, Chen G, Chen P, Zhou L. A Gaussian type-2 fuzzy programming approach for multicrowd congestion-relieved evacuation planning. IEEE Trans Intell Transport Syst 2022;23:20978–90.
[54] Jiang P, Men J, Xu H, Zheng S, Kong Y, Zhang L. A variable neighborhood search-based hybrid multiobjective evolutionary algorithm for HazMat heterogeneous vehicle routing problem with time windows. IEEE Syst J 2020;14:4344–55.
[55] Deb K, Jain H. An evolutionary many-objective optimization algorithm using reference-point-based nondominated sorting approach, part i: solving problems with box constraints. IEEE Trans Evol Comput 2014;18:577–601.
[56] Veček N, Črepinšek M, Mernik M. On the influence of the number of algorithms, problems, and independent runs in the comparison of evolutionary algorithms. Appl Soft Comput 2017;54:23–45.
[57] GB/T37243-2019, Determination method of external safety distance for hazardous chemicals production units and storage installations, in, State Administration of Market Regulation, Beijing, 2019.